Laser and Particle Beams (2006), *24*, 131–141. Printed in the USA.

DOI: 10.1017/S0263034606060204

Charge state of Zn projectile ions in partially ionized plasma: Simulations

ERAN NARDI,[1] DIMITRI V. FISHER,[1,4] MARKUS ROTH,[2] ABEL BLAZEVIC,[2] AND DIETER H.H. HOFFMANN[3]

[1]Faculty of Physics, Weizmann Institute of Science, Rehovoth, Israel
[2]Institut für Angewandte Physik, TU-Darmstadt, Germany
[3]Gesellschaft für Schwerionenforschung mbH, Darmstadt, Germany
[4]Soreq NRC, Yavne, Israel

(Received 1 July 2005; Accepted 19 September 2005)

Abstract

This study deals with the simulation of the experimental study of Roth *et al.* (2000) on the interaction of energetic Zn projectiles in partially ionized laser produced carbon targets, and with similar type experiments. Particular attention is paid to the specific contributions of the K and L shell target electrons to electron recombination in the energetic Zn ionic projectile. The classical Bohr–Lindhard model was used for describing recombination, while quantum mechanical models were also introduced for scaling the L to K cross-section ratios. It was found that even for a hydrogen-like carbon target, the effect of the missing five bound electrons brings about an increase of only 0.6 charge units in the equilibrium charge state as compared to the cold target value of 23. A collisional radiative calculation was employed for analyzing the type of plasma produced in the experimental study. It was found that for the plasma conditions characteristic of this experiment, some fully ionized target plasma atoms should be present. However in order to explain the experimentally observed large increase in the projectile charge state a very dominant component of the fully ionized plasma must comprise the target plasma. A procedure for calculating the dynamic evolvement of the projectile charge state within partially ionized plasma is also presented and applied to the type of plasma encountered in the experiment of Roth *et al.* (2000). The low temperature and density tail on the back of the target brings about a decrease in the exiting charge state, while the value of the average charge state within the target is dependent on the absolute value of the cross-sections.

Keywords: Charge state of projectile ions; Collisional radiative code; Laser produced plasma; Monte Carlo simulations; Particle beam interaction with plasma

1. INTRODUCTION

The charge state of energetic ions interacting with solid or gaseous matter as well as with a completely or partially ionized plasma target has been the subject of a considerable amount of attention both theoretical and experimental. It was predicted theoretically (Nardi & Zinamon, 1982) that the charge state of such ionic projectiles should be significantly higher than for the same projectile species interacting with a cold target. The total absence of bound electrons in the fully ionized plasma is the reason attributed to the occurrence of the much higher charge state. The high charge state strongly affects the range and shape of the energy deposition curve bringing about a dramatic range shortening effect in the plasma. The basic predicted effects were verified experimentally in beam plasma interaction experiments at the heavy ion accelerator at the Gesellschaft für Schwerionenforschung (GSI) (Hoffmann *et al.*, 1990; Jacoby *et al.*, 1995).

Recently conducted experiments on the interaction of high energy Zn ions at 5 MeV/A, with a laser produced partially ionized carbon target (Roth *et al.*, 2000) are the subject of the present paper. Charge transfer to the high Z projectile ion from the bound electrons of the low Z target in condensed matter or in plasma, provides an efficient channel for the reduction of projectile ion charge state. In fully ionized targets, this channel is absent thereby accounting for the significantly higher charge state. Thus, the average charge of the projectile, in the partially ionized target, should not be as high as for the case of a completely ionized plasma target but intuitively larger than for a cold target. It is therefore of much interest to study the case of partially ionized targets, intermediate between a fully ionized and cold target.

Address correspondence and reprint requests to: Eran Nardi, Department of Physics, Weizmann Institute of Science, Rehovoth 76100, Isreal. E-mail: eran.nardi@weizmann.ac.il

At this stage Roth *et al*. (2000) measured the energy deposition only, in partially ionized laser produced plasma which they surmised was predominately helium-like. These authors concluded that for the condition of the above experiment, the effective charge state for stopping, Z_{eff}, of the Zn ions is higher by four charge units in the partially ionized plasma compared to the cold target. Their analysis was based on obtaining a consistent picture for the energy loss.

The purpose of the present paper is to investigate theoretically by means of simulation, this experiment of Roth *et al*. (2000) dealing with the partially ionized targets and apply the basic methods in future to similar type experiments. The bound electron recombination process into the projectile is stressed here and in particular the contribution of the different target atomic shells to bound electron recombination. Recently, Maynard (2002) and Maynard *et al*. (2000) calculated the Zn charge state in a Helium-like carbon target and found essentially no difference between this result and that for a cold gas target. These authors used the classical trajectory Monte-Carlo method (CTMC).

In this paper, we in addition give attention to the atomic structure of the target atoms by employing the Rehovoth detailed collisional radiative (CR) code (Fisher & Maron, 2003). This code predicts that for the conditions representative of the target in the experiment of Roth *et al*. (2000), various ionization stages including fully ionized carbon are present in the target. The charge equilibrium charge state of the energetic Zn projectile ions is studied for some of these multi-ionization stage targets, as well as for the hydrogen-like and helium-like targets. In this paper, we report results obtained under the assumption of local thermodynamic equilibrium (LTE) at any point within the target plasma. The non-LTE analysis is currently being studied.

Finally, an essential point in the present paper is the description of a procedure for the dynamic calculation of the evolving charge state of the ionic projectile penetrating laser produced plasma target. The target is divided into small enough intervals within each of which the atomic structure of the target is obtained on the basis of the CR code calculations. Within each interval, the change in projectile charge state is determined using the Monte Carlo method. Attention is also given to the effect of the plasma tail on the rear side of the target on the exiting charge state as well as to the absolute cross-section values. The difference between the ionic charge states within the target compared to that exiting it is examined and discussed.

In Section 2, we deal with the basic theory as well as the method of calculation. In Section 3, the results are presented both for equilibrium and non-equilibrium charge states, while in Section 4 we conclude.

2. THEORY AND CALCULATIONS

The charge state of the energetic Zn projectile at 5 MeV/u interacting with the carbon gas and with the plasma target is determined in the present calculations by the competition between projectile electron ionization and electron recombination as the ionic projectile traverses the target. A detailed account of this procedure has very recently been given (Nardi *et al*., 2002), although for problems dealing with energetic cluster target interactions with solids.

2.1. Ionization cross-section

The single electron ionization cross-section was determined in previous work (Nardi & Zinamon, 1982; Nardi *et al*., 2002) using the classical binary encounter approximation (BEA) (Richard, 1985). This approximation assumes a classical two body interaction between the individual bound projectile electron and the target nucleus, disregarding the other projectile electrons during collision. The cross-section for the ionization of a projectile electron bound by the energy U_n is given by,

$$\sigma_I = (\pi e^4 Z_t^2/U_n^2) G(V), \tag{1}$$

where, $G(V)$ is a function of V, the scaled projectile velocity v/v_n, v is the projectile velocity and v_n the orbital velocity of the bound electron. $G(V)$ was calculated (McGuire & Richard, 1973), and is based on detailed classical binary collision scattering calculations (Gryzinski, 1965). Z_t denotes the effective charge of the screened target nucleus for projectile ionization; see below, where the additional ionization due to the target electrons is also mentioned.

We compare here as an example, the experimental cross-section (Xu *et al*., 1988) for the single K shell ionization cross-section in 8.6 MeV/amu Ca^{18+} ions with a Nitrogen target to the BEA cross-section. The experimental result is $(12 \pm 2)\ 10^{-20}$ cm^2/at, while the BEA result which is 30% higher than experiment gives 1810^{-20} cm^2/at, in satisfactory agreement. The general situation however is more complex. The calculated BEA cross-sections were found for example, to be too small to account for experimental results in recent GSI work on heavy ion plasma studies. Dietrich *et al*. (1992) introduced a factor of 2.5 by which the BEA cross-sections were multiplied. These authors attribute this effect partly to Auger cascades following inner-shell ionization. Also, the CMTC model for the calculating ionization cross-sections was used, and gave higher cross-sections compared to the BEA ones, (Stockl *et al*., 1998).

An important process that must be accounted for and which has recently been the subject of discussion in connection with heavy ion fusion is that of multiple electron ionization (Mueller *et al*., 2002). Although not as importance in the case studied here, compared for example to Ar at 10 MeV/u on N, we feel that it is worthwhile to mention this effect. As a result of multiple ionization, the charge state of the ion beam increases more than would be the case if only a single electron were lost in each encounter. DuBois *et al*. (2004) have very recently measured multiple electron loss from 1.4 MeV/amu U ions of charge state 4 to 10, while also summarizing experimental data which also included highly

stripped ions. These authors find that the charge states in the range of 4 to 10 behave in a regular manner, while for the higher charge state projectiles, the cross-sections exhibit large variations as a function of projectile charge. One apparent property observed is the increase of the relative multiple ionization cross-sections with decreasing projectile charge state and energy, as well as with increasing target atomic number (Meyerhof *et al*., 1987; Meuller *et al*., 2002). An experimental result due to the latter authors dealing with 10 MeV Ar^{+6} ions interacting with nitrogen target is relevant to the case of the Zn ion beam studied here. These authors found that the two electron stripping cross-section is 0.83 of the single ionization cross-section. Due to the complexity and to the lack of detailed knowledge regarding the projectile ionization cross-sections as outlined above; the BEA cross-section was multiplied by a constant factor of three and the influence of this scaling of the cross-section on the results was studied in the dynamic charge state calculations.

In the calculations in the present paper, for each ionization stage of the energetic projectile, the eigen-energies are calculated for each atomic shell. The ionization cross-section is obtained by summation over all the atomic shells. The effective target charge state for ionization for the relatively high energy of 5 MeV/u Zn ion for a cold target is $Z_t^2 + Z_t$ (Shevelko *et al*., 2001) where Z_t is the nuclear charge of the target atom and the linear term in Z_t is due to the bound target electrons in the cold target. For ionized targets this term becomes the number of remaining bound target electrons while the additional ionization due to the free electrons must be added. It was found that the linear term well approximates the situations encountered here. The above quoted expression is valid at energies higher than those encountered here; however the uncertainties within the ionization cross-section are treated by examining the behavior of the results using the scaling factor mentioned above as well as by the calibration of the recombination cross-section, see below.

2.2. Electron recombination cross-section

The cross-section employed here for recombination is the classical Bohr–Lindhard model (Bohr & Lindhard, 1954) which is still in current use for the description of recombination for example (Assmann *et al*., 1999) and was shown to account fairly well for measured capture cross-sections for highly charged ions (Knudsen *et al*., 1981). This model, which is based on rather rough approximations, yields the recombination cross-sections for the different target shells, which is basic for dealing with the problem at hand.

In essence, the model is based on two ion-atom interaction distances: The first R_1, the distance of release, is determined as the distance where the force exerted by the projectile on the bound electron is equal to the electron atomic binding force F_a, thus for the projectile charge of Z_p,

$$Z_p e^2/R_1^2 = F_a. \tag{2}$$

The second is the distance of capture R_c, where for distances less than R_c the potential energy of the released electron in the field of the projectile exceeds the kinetic energy of the electron in the frame of the ionic projectile. Bohr and Lindhard (1954) assume that due to the violent projectile electron collision the bound electron velocity is greatly reduced during the gradual loosening of the atomic binding. They make the approximation that after the completion of the release process, the velocity of the electron relative to the ionic projectile will be that of the projectile. Thus,

$$Z_p e^2/R_c = 1/2\ \mathrm{mV}^2, \tag{3}$$

where V is the projectile velocity and m the electron mass. When $R_1 < R_c$, release and capture occur and the capture cross-section σ_c is simply given by,

$$\sigma_c = \pi R_1^2. \tag{4}$$

The situation is more complicated for $R_1 > R_c$, if release occurs instantaneously, the capture cross-section would be zero. Release however according to Bohr and Lindhard (1954) is a gradual process whose probability per unit time of the order of v/a, where v is the atomic electron velocity, and a the bound electron radius. The time during which capture occurs is roughly R_c/V. Thus the probability that a released electron be captured is roughly $(v/a)/(R_c/V)$ and the cross-section for capture based on these approximations is given by,

$$\sigma_c = \pi R_c^2 (v/a)/(R_c/V). \tag{5}$$

The cross-section was integrated over the target electron shells assumed to be composed of simple Bohr orbitals and not by adopting a more detailed electron distribution as for example in (Knudsen *et al*., 1981).

Although the Bohr–Lindhard model yields good first approximations to absolute magnitude recombination cross-sections (Knudsen *et al*., 1981), the absolute value of the cross-section must be adjusted in order to fit experimental data of the type described here, this will be done below. It is appropriate to add here that the quantum models can differ from experiment by more than a factor of two and this is for the simpler case of a totally ionized projectiles (Sols & Flores, 1989). Another point pertinent to the discussion below is the prediction based on Eq. (5), that σ_c should increase with binding energy of the target electron. This follows since the atomic electron radius of the Bohr orbital contracts with increasing binding energy. This phenomenon is more complicated for the more detailed electron distribution model of Knudsen *et al*. (1981) for example.

In addition to the Bohr–Lindhard model, quantum mechanical models are also alternately used for determining the relative contribution to recombination between the K shell and L shell electrons as well as for the variation in the mag-

nitude of σ_c of the K shell with the increase in binding energy. The first model (Meyerhof *et al*., 1985) is based on the relativistic eikonal approximation. Rozet *et al*. (1996) have recently applied this model for the calculation of recombination in their program for calculating charge states of high energy ionic projectiles. The second model (Lapicki & McDaniel, 1980) is also currently used in the study of heavy ion collisions. This model is and has been used extensively in calculating the K, L, and M, X-ray yields in heavy ion collisions and is essentially based on the Oppenheimer Brinkman Kramers (OBK) formulation of Nikolaev (1967). The third model used is the OBK theory without the eikonal corrections (Betz, 1981) which gives the cross-section for n_i, the initial state quantum number to n_f, the final quantum state number. The states are assumed to be hydrogen-like and the cross-sections are averaged over 1 m.

2.3. K shell population and collisional radiative code

Since for the problem at hand the K shell is the primary contributor to recombination, the K shell occupancy is of major importance. For the laser produced target plasma in the Roth *et al*. (2000) experiment, this is determined using the detailed CR code for carbon (Fisher & Maron, 2003). With the aid of the code we determine the respective abundances of carbon ions with 2, 1, or 0 electrons in the K-shell. Briefly, the code is based on the formalism of effective statistical weights of bound states in plasma, (Zimmerman & More, 1980; Fortov & Yakubov, 1990; Fisher & Maron, 2002) and is applicable to plasmas with ion densities up to near solid value. The code utilizes the extensive databases for collisional and radiative processes compiled at the Weizmann Institute Plasma Laboratory (Arad *et al*., 2000; Ralchenko & Maron, 2001). The code performs time-dependent CR composition calculations; it is used for steady state and LTE calculations as well. We emphasize that the present code (Fisher & Maron, 2003) describes bound states of every ionization stage of carbon, and accounts self-consistently for the simultaneous presence of all ionization stages of carbon in the plasma. Therefore, bound state populations and ionzation-stage composition of the plasma can be studied in detail. The code is executed for carbon only and does not account for the presence of Zn ion, and no description of doubly-excited states is included in the code. Thus, abundance of ions with no electrons in the K-shell is evaluated as a sum of abundances of CVI and CVII minus the abundance of CVI ground state. Abundance of ions with one electron in the K-shell is given by the sum of abundances of CVI ground state and CV excited states (the latter being the total abundance of CV minus the abundance of CV ground state). Abundance of ions with two electrons in the K-shell is given by the sum of abundances of CI, CII, CIII, CIV, and of the ground state of CV.

2.4. Elements of the Zn projectile charge state calculation

The ion track is divided into sufficiently small path lengths, such that the probability of projectile charge change does not exceed 0.1 within the given path length. The increase or decrease of the charge state of the projectile within the path interval is determined by means of the Monte Carlo method. The energy loss and scattering of the projectile as it traverses the foil are neglected.

3. RESULTS

In the present section two types of investigations will be described. First equilibrium charge state distributions will be determined for different carbon target configurations, where these differ regarding their K and L shell population occupancy. The ionization cross-section employed here is the single ionization BEA cross-section, while the recombination cross-section is scaled to obtain the correct experimental result as known for the cold gas target. In this context the equilibrium projectile charge state in a carbon gas Z_{gas} and the effective charge for stopping Z_{eff} should be discussed. In the Roth *et al*. (2000) experiment Z_{eff} for the stopping and not Z_{gas} was measured. Data showing that in a gas target the projectile charge state is well approximated by Z_{eff}, for projectile atomic numbers less than 50 and for energies from 1 to 10MeV/A was presented (Maynard *et al*., 2000). Thus for cases of the Zn projectile at 5 MeV/A, dealt with here, we make the assumption that the equilibrium charge state within the gas Z_{gas} is essentially equal to Z_{eff}.

In the second set of results a dynamical charge state calculation is described, where the target simulates laser produced plasma as in the experiment of Roth *et al*. (2000). In this procedure in each interval the plasma target atomic configuration is determined on the basis of the CR model results. It is important to add that density effects on projectile-plasma interaction, which could become of importance for target densities of the order of 10^{21} cm^{-3} (Maynard, 2002) were neglected here. The projectile was assumed to be in its ground state, an assumption valid for almost the entire traversed target. Future work will bring the density effect into account.

3.1. Projectile charge state equilibrium calculations

3.1.1. Cold low density carbon target

As a first step, we calculate the charge state of the Zn projectile in a cold carbon, low density target, where all the atomic shells are fully occupied, and where density effects do not come into play. The quantity of interest here is the equilibrium charge state. The dynamical evolvement of the charge state will be presented below for plasma targets. The statistical fluctuations in the results are large (these fluctuations manifest themselves in the finite width of the observed charge distribution). By averaging over 500 different simulations, the average equilibrium charge state

obtained is 23.0 with a standard deviation (SD) of 0.7. This agreement with Roth *et al*. (2000) for a cold target was obtained as discussed above, by multiplying the Bohr–Lindhard recombination cross-section (Bohr & Lindhard, 1954) by an appropriate scaling factor, equal here to 0.56. If one were to assume that the Bohr–Lindhard model gives correct absolute values, than the BEA ionization cross-sections is accordingly too small as was pointed out above (Dietrich *et al*., 1992; Stockl *et al*., 1998). Apart from this, the model is parameter free and is used to obtain the contribution of the different target shells at the different ionization stages.

An essential point in the problem dealt with here is the relative contribution of the L to K shells of the target atoms to recombination. The Bohr–Lindhard recombination model yields an L shell recombination cross-section which is about 0.09 of the corresponding K shell cross-section, for the Zn ion at a charge state in the vicinity of 20. This ratio according to Meyerhof *et al*. (1985) is higher by about a factor of 2 as compared to Bohr–Lindhard. The L to K recombination cross-sections according to the two other quantum mechanical models are extremely small in these cases and the L shell cross-section according to them can be neglected (Lapicki & McDaniel 1980; Betz, 1981). The discrepancy between these models and that of Meyerhof *et al.* deserves further consideration.

The projectile charge state was also calculated adjusting the ratio of the L to K recombination cross-section in accordance to Meyerhof *et al*. (1985) by multiplying the Bohr–Lindhard L shell cross-section by a factor of 2, and retaining the value of the K shell cross-section. The cold target now gives an average equilibrium charge state of 22.9 with a SD of 0.7, indicating the lack of sensitivity of recombination to the L shell. Finally by assuming a negligible L shell recombination cross-section in accordance with (Lapicki & McDaniel, 1980; Betz, 1981) the equilibrium projectile charge state in this cold target is 23.1 with an SD of 0.7.

3.1.2. Helium-like-carbon target

The laser produced plasma in the experiment of Roth *et al.* (4) according to these authors, should contain carbon ions where only the K shell electrons are populated, thus with a target charge state of +4. The target plasma density according to Roth *et al*. (2000) goes up to 10^{21} e/cm^3, while the plasma temperature can reach 60 eV. These conclusions of the plasma conditions were based on time resolved plasma spectroscopy and confirmed by computer simulation of laser plasma interactions. In the following sections, the electronic structure of the target ions for the conditions pertinent to the experiment will be studied by us in somewhat more detail using the Rehovoth CR code, and the results will be applied to the present problem.

At first we study the Helium-like target carbon target plasma. In calculating the electron recombination cross-section, the 4 L shell electrons are not present, thus not contributing to recombination. On the other hand, the missing L shell electrons bring about an increase in the K shell binding energy compared to the cold target case. Increasing the binding energy results in an increase of the K recombination cross-section as discussed above. Table 1 gives the binding energies as well as the relative K shell recombination cross-sections based on the different recombination models, as a function of the target degree of ionization, for the fragment with the relevant charge of 22. Although not the same, the recombination cross-section ratios for the various models follow the same pattern, with the cross-section increasing as the degree of target ionization increases. Calculating the charge of the Zn projectile for the Helium-like target, once more by averaging over 500 simulations and using the Bohr–Lindhard recombination model, we obtained the equilibrium average charge state of 22.5, with SD = 0.7, a decrease, not an increase, in the projectile charge state from the cold target value of 23. This effect was noted previously by Maynard (2002). We note that assuming incorrectly that the binding energy of the K shell for the Helium-like target is that of the cold target, the projectile charge state increases to 23.1 as noted above.

3.1.3. Hydrogen-like target

The dominant role played by the K shell in electron recombination has been demonstrated above when dealing with the cold target. In the following we calculate the charge state of the energetic Zn projectile when only one electron occupies the K shell of the carbon plasma atom. As will be seen below the hydrogen-like target atoms should have a substantial presence in the plasma target of the Roth *et al*. (2000) experiment.

For the hydrogen-like carbon target, the K shell binding energy is higher than for the Helium-like and cold target, respectively, see Table 1, where the K shell recombination cross-sections are also given for these three targets. Although the K shells recombination cross-section further increase

Table 1. *Average equilibrium projectile charge state, Z_p as a function of K and L shell target population. Also given are the K shell bonding energies and relative K shell recombination cross-sections, normalized to unity for a carbon target with completely full shells, for each of the recombination models. The representative projectile is 22 times ionized Zn (Zp = 22). B&L is the Bohr–Lindhard (Bohr and Lindhard, 1954) theory, and OBK is as given by Betz, (Betz, 1981) and while M. is according to (Meyerhof et al*., 1985).

				σ_K(relative)@$Zp = 22$		
Z_p	# K shell	# L shell	$K_{bin.}$(eV)	B&L	OBK	M
23.0	2	4	291	1.0	1.0	1.0
22.5	2	0	386	1.3	2.0	1.6
23.6	1	0	489	1.7	3.6	2.2
28.0	0	0				

with respect to the Helium and a cold target case, the presence of only one K shell electron causes an effective decrease in the recombination cross-section. The average equilibrium charge state obtained here increase relative to the cold target to 23.6, with SD = 0.8, a rather small increase compared 23 for the cold target.

To summarize, the above results show that the average equilibrium projectile charge state is within a range of 22.5 to 23.6 for any number of bound K shell electrons, far from the experimentally determined value of 27 for the assumed partially ionized plasma. We note as before, former value was obtained by Roth *et al*. (2000) on the basis obtaining a consistent picture for the energy loss. Indeed, making different assumptions regarding the plasma temperature and density could alter the calculated energy loss and with it the value of the charge state.

In Table 1, the equilibrium charge for the completely ionized target with no electrons in the K and L shell is given. The equilibrium charge in this case is 28, since the probability of projectile K shell ionization is very small due to the large binding energy of these electrons.

3.1.4. Results of CR model and mixed targets

Based on the above discussion, the critical quantity which determines the large experimental difference in the average equilibrium charge state is the probability for total absence of bound electrons. In Figure 1, results obtained using the CR model described above, for the K shell population at LTE, are plotted as a function of temperature for the carbon plasma densities of 10^{19}, 10^{20}, and 10^{21} ions/cm^3. These densities are typical to the experiment of Roth *et al*. (2000). The projectile charge state calculation proceeded basically as described above using the Monte Carlo method. However, in these mixed targets, which contain a variety of atomic species, the target electron configuration can contain 0, 1, or 2 bound electrons in the K shell.

For a target plasma at the density of 10^{20} ions/cm^3, and temperature 50 eV, about 0.7 of the target ions possess one K shell electron, while in 15% of the cases the K shell is completely empty and in the other 15% the K shell is full with two electrons. Carrying out the calculation as outlined above, the average equilibrium charge state of the Zn projectile ion is here 23.9 with SD of 0.8 charge units. This result is only about one charge state unit higher than for a cold target and quite different from the plasma produced target as determined by Roth *et al*. (2000).

At 10^{19} ions/cm^3 and $T = 50$ eV, the number of completely ionized target atoms is equal in number to that of the target ions with one K shell electron, that is, with no cases of two electrons in the K shell. For this target, corresponding to about 0.510^{20} e/cm^3, the equilibrium charge state for the 5 MeV/u Zn projectile was found to be equal to 25.0, with a SD of 0.8, and not within the range of the experimentally determined charge state of Roth *et al*. (2000) found to be 27, a value obtained, based on a consistent analysis of the energy loss.

In the same manner, assuming a more highly ionized target where 0.75 of the target atoms are completely ionized while 0.25 posses one bound K shell electron, the average equilibrium charge state here is 26.1 with a SD of 0.7, almost within the bounds of the Roth *et al*. (2000) experiment. These conditions are representative of carbon plasma at 10^{19} ions/cm^3 and at a temperature of about 60 eV.

Figure 2 gives the average equilibrium charge state along with the standard deviation for a mixture of hydrogen-like and completely ionized carbon, as a function of the percentage of completely ionized carbon. In order to obtain the experimental results of Roth *et al.* (2000), the plasma must be approximately 80% fully ionized. These conditions differ substantially from the Helium-like target configuration. Further experimentation and also direct measurements of the charge state, coupled with calculations would therefore be of much interest see below.

3.2. Non-equilibrium projectile charge state calculations

In the present section we simulate the dynamic interaction of the 5 MeV/A Zn beam with a plasma target similar to the laser produced plasma obtained in the experiment of Roth *et al*. (2000). The dynamic evolvement of the charge state as the beam traverses the target is calculated. The target used here is a somewhat idealized version of the experimental one as given by Roth *et al*. (2000) and the temperature and density profiles are presented in Figure 3. We note that the peak temperature is at 60 eV. An important feature in Figure 3 is the temperature and density tails on the back side of the target. The influence of this region, where the K shell population increases, on the charge state of the ion emerging from the target is observed in the results presented below. The target intervals were chosen such that the probability for ionization or recombination does not exceed 10%. As noted above, in each interval the atomic structure was determined based on the collisional radiative data and the recombination cross-section was accordingly calculated.

In Figure 4a, the charge state as a function of penetration depth is presented for the Zn projectile. The results were averaged over 1000 projectiles traversing the target and the SD due to statistical fluctuations is 1.3 charge units. The ionization cross-section for the results with the slower rise time was obtained using the BEA as in Eq. (1). The results with the more rapid rise time were obtained assuming that the ionization cross-section is due to the BEA multiplied by 3, this account for the effects out-lined above when discussing the ionization cross-section. In the latter case, the recombination cross-section was also multiplied by this factor in order to obtain the correct cold target equilibrium charge state. The different assumption regarding the magnitude of the cross-sections also result in a small difference in the charge state of the emerging ions as well as a difference in the rise time. A more significant difference lies in the average charge state of the Zn ion as it traverses the target.

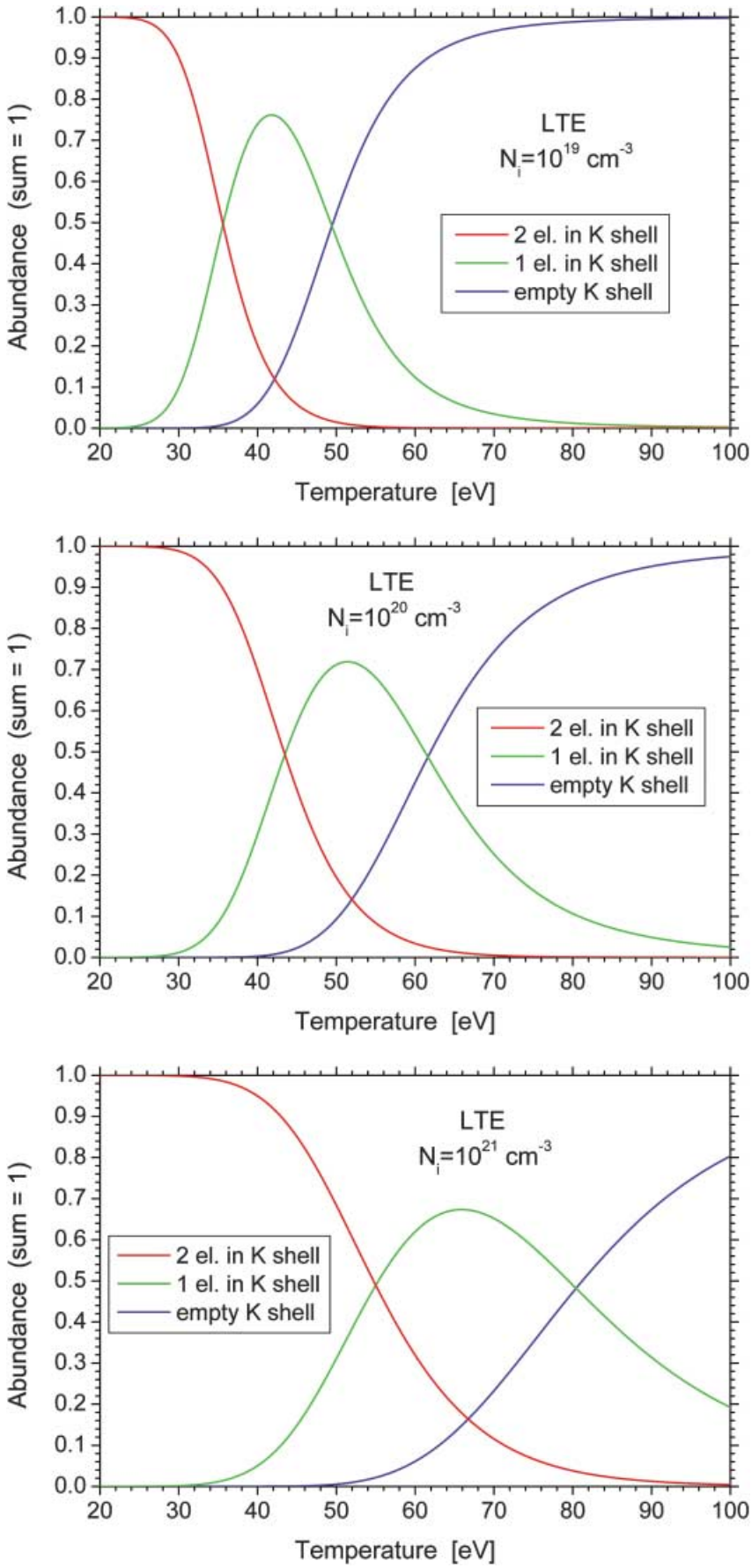

Fig. 1. Number of electrons in the K shell as a function of temperature at LTE, for three different carbon plasma densities. Results from calculations using the collisional radiatiative code (Fisher & Maron, 2003).

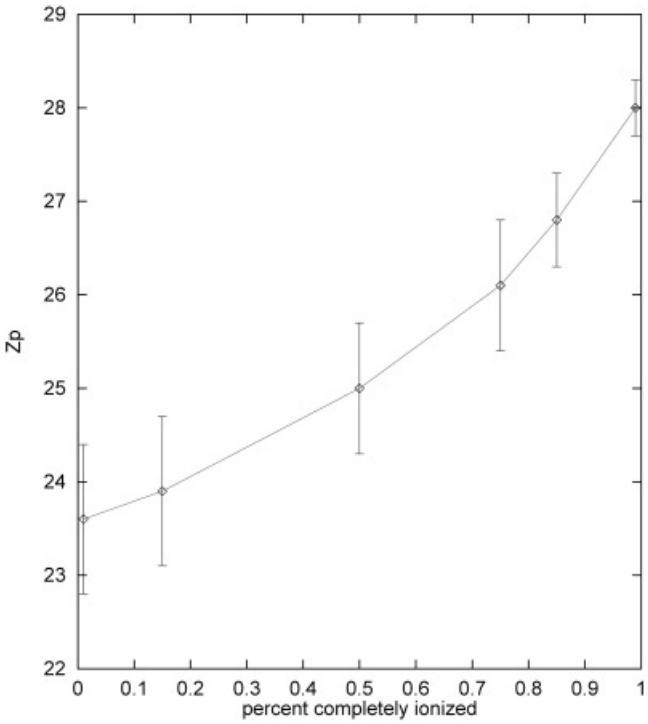

Fig. 2. Average equilibrium charge state of Zn projectile ion at 5 MeV/A in a plasma consisting of a mixture of fully ionized carbon target atoms and hydrogen-like carbon ions. The x axis gives the percentage of the fully ionized component.

Assuming as noted above, that the charge state is essentially the same as the effective charge for stopping, the difference in the average charge state within the target, will manifest itself in the stopping power of the ion. For the lower magnitude cross-section, the average charge is 22.9, while for the higher cross-sections it is 23.4. Both values are however significantly smaller than the value of 27 as measured by Roth *et al*. (2000) and as stressed here were based on the consistency of the energy loss data.

With the latter conclusion in mind, we have rescaled the temperature distribution of Figure 3 such that the peak temperature is 100 eV significantly higher than the 60eV upon which the results of Figure 4a are based. In Figure 4b, we present the projectile charge state for the higher temperature distribution. The average charge within the target charge based on the BEA cross-section of Eq. (1) is 24.8 while by multiplying the ionization and recombination cross-sections by the factor of three we obtain the average charge state of 26.1, approaching the experimental result of 27. A striking feature in Figure 4b is the significant decrease of the exiting charge state, which in the case of the higher cross-section values, attains a value of about 5.2 charge state units. The decrease is significantly smaller for the cross-sections based on Eq. (1) which is 3 charge units. These results give significance to the simultaneous study of the charge state by means of energy deposition and by the direct measurement of the exiting charge state.

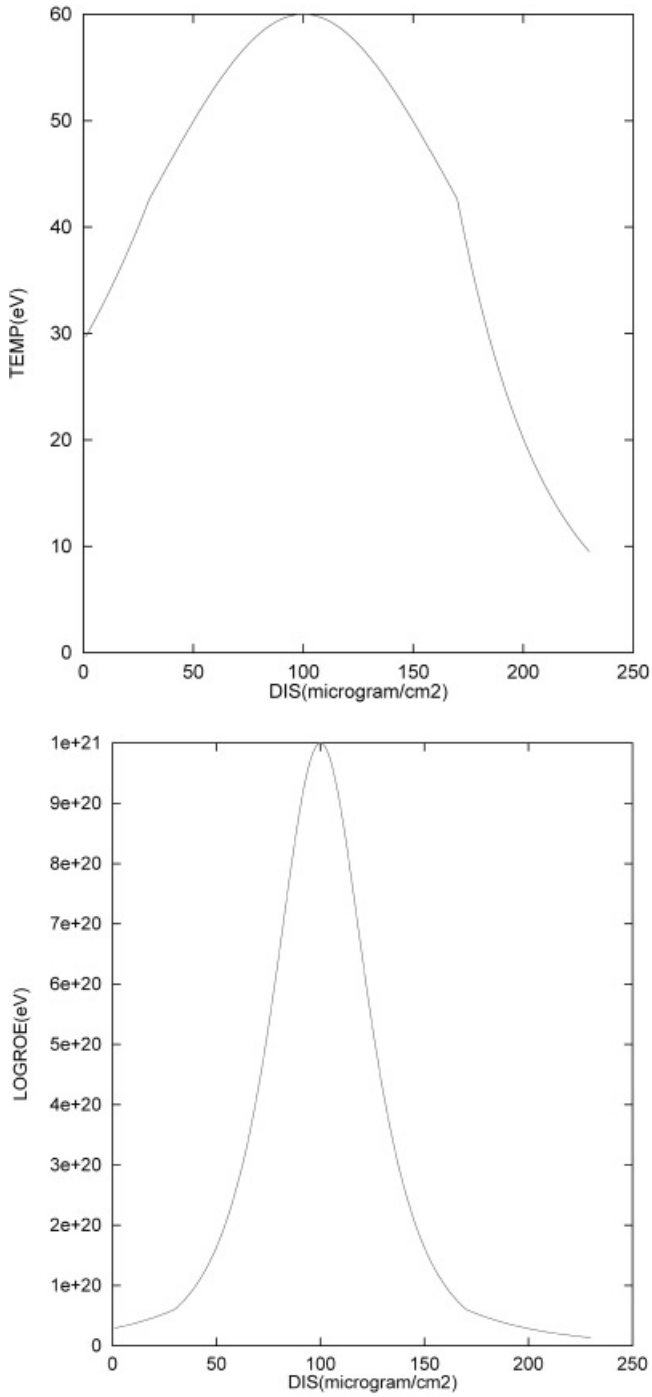

Fig. 3. Temperature and density profiles representing very roughly a laser produced plasma of 1 micron thickness. The ion beam is incident from the left.

4. CONCLUSIONS

We have simulated here the charge state of 5 MeV/u Zn ions interacting with a variety of partially ionized carbon targets as well as for cold and completely ionized carbon. The purpose of these calculations was to analyze the results of experiments of Roth *et al*. (2000) and future similar type

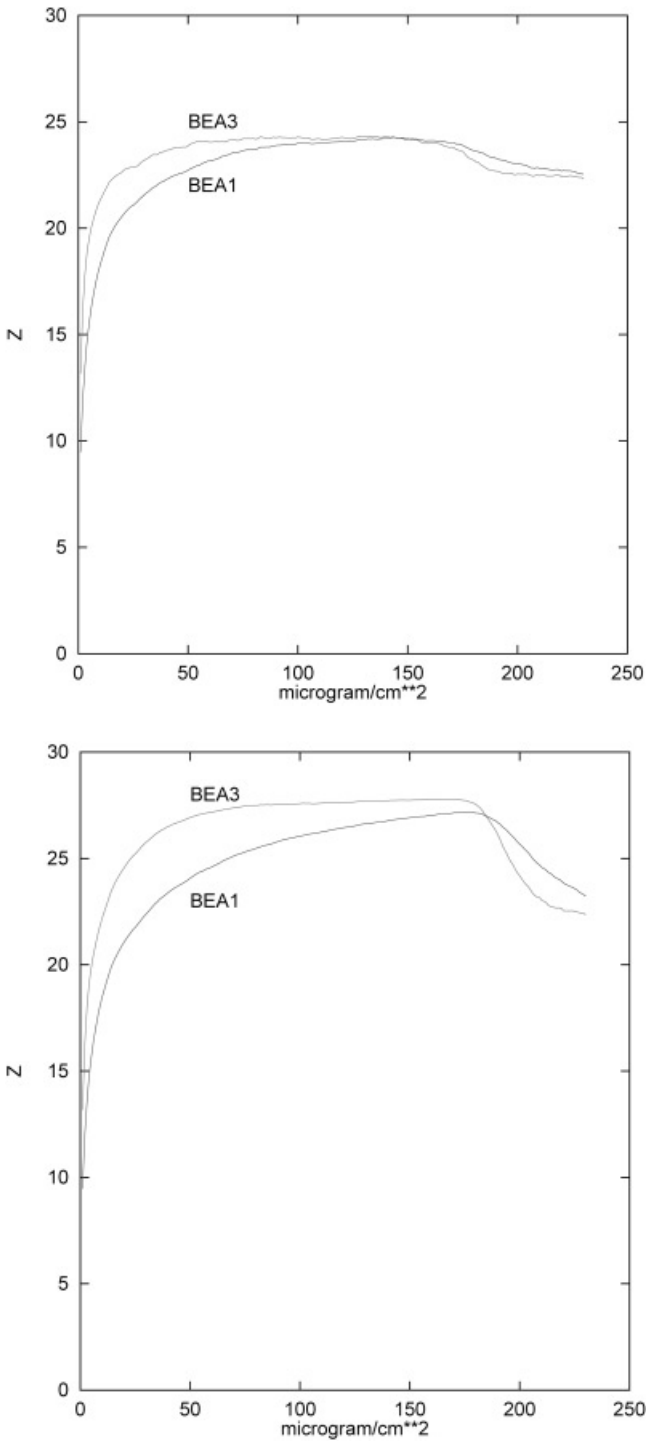

Fig. 4. (**a**) Average charge state as a function of penetration depth for a Zn ion at 5 MeV/A incident on the plasma represented in Figure 3, where the plasma temperature peaks at 60 eV. The results are averaged over 1000 events. BEA1 indicates calculations using the BEA cross-section of Eq. (1), while BEA3 denotes results for which the BEA and recombination cross-sections were multiplied by 3. (**b**) Average charge state as a function of penetration depth for a Zn ion at 5 MeV/A incident on the plasma represented in Figure 3, but with the temperature multiplied by 5/3, such that the peak temperature is 100 eV. The results are averaged over 1000 events. BEA1 indicates calculations using the BEA cross-section of equation 1, while BEA3 denotes results for which the BEA and recombination cross-sections were multiplied by 3.

experiments, dealing with the measurement of the projectile charge state interacting with partially ionized laser produced carbon plasma targets. The basic model used for bound electron–ionic projectile recombination is the classical Bohr–Lindhard model (Bohr & Lindhard, 1954). Quantum mechanical models were also used to scale the magnitude of the L to K shell recombination cross-sections, as well as for investigating the dependence of the cross-section on target electron binding energy.

Since L shell electrons are stripped from partially hot target atoms, it was of interest to study the contribution of the L shell bound electrons to recombination. For the energetic Zn projectile studied here it was found, that for cold targets, recombination due to L shell electrons is essentially negligible.

Helium-like and hydrogen-like carbon target atoms were also studied. In both cases the recombination cross-section per target electron were found to be larger than for the K shell electron in the cold target, this effect being due to the increase of the binding energy with ionization. For the Helium-like target the average equilibrium charge state is half a unit less than for the cold target while for the hydrogen-like target the charge state is only 0.6 units of charge higher than for the cold target.

In order to obtain a significant shift in the projectile charge state from the cold target value, as observed in the experiment by Roth *et al*. (2000), the target must therefore consist of an appreciable fraction of completely ionized target atoms The atomic structure of the target was studied in detail using the detailed Rehovoth collisional radiative code (Fisher & Maron, 2003), the results of which give, as the density decreases and the temperature rises, an increasing percentage of totally ionized plasma. Average equilibrium charge states were calculated for mixed targets made of different ionization stages representing various plasma conditions. These results lead to the conclusion that in order to explain the energy loss measured by Roth *et al*. (2000), a significant amount of completely ionized carbon must be present in the target.

Most relevant to the analysis of the experiment are the dynamic calculations dealing with the evolving charge state of the Zn ion penetrating a representative laser plasma target, whose temperature and density vary with penetration depth. The calculation employs the collisional radiative code (Fisher & Maron, 2003) which gives the target K shell electron occupancy as a function of the penetration depth, based on which the temperature and density dependent recombination cross-section is calculated. Targets with peak temperatures of 60 and 100 eV were studied using the cross-sections based on Eq. (1) as well as for the case of the ionization and recombination cross-sections both multiplied by 3. Of particular interest is the influence of the temperature and density tail at the rear side of the target on the value of the charge state. The tail brings about a decrease in the exiting charge state, in relation to the central portion of the target. This effect, which complicates charge state analysis

within the bulk of the target, is particularly pronounced for the higher temperature target, where the higher absolute value cross-sections are also employed. In this case, the decrease in the exiting charge state is 5.2 units. This effect could however, on the other hand, shed light on the plasma tail structure. Another point worth mentioning is the influence of the scaled absolute magnitude of the cross-sections on the average charge of the projectile within the target. The square of this quantity is representative of the energy loss of the Zn ion traversing the target. For the 60 eV target the cross-section based on Eq. (1) yields an average charge state of about half a unit lower than that obtained employing the cross-sections which were multiplied by a factor of 3. For the 100 eV plasma target, a difference of 1.3 charge units was obtained between the no scaled and scaled cross-sections.

The present paper can be viewed as an initial step in the analysis of projectile charge states in partially ionized plasma. Such studies must be carried out in tandem with experimental work dealing with charge state measurements, as well as detailed diagnostics of the plasma target. The results of the present work and the comparison to the experimental work of Roth *et al*. (2000), demonstrate that much is still to be resolved, and that future experiments and theoretical analysis are very desirable. In particular, in connection with the experiment dealt with here and according to the present analysis, the target temperature could well be in the region of 100 eV. Of particular value would be a direct measurement of the exiting charge state together with the energy loss in this and in other combinations of projectiles and partially ionized targets. Experiments which would complement the study of Roth *et al.* (2000) should in our opinion also deal with situations where the greater part of the cold recombination cross-section originates from the L shell. Low energy C shell ions at 2 MeV provide for such a situation.

A large range of applications depends on the details of energy deposition profiles of ions in matter, and here the charge state of the ion inside the bulk target material is of utmost importance. Among them, high energy density physics (Hoffmann *et al*., 2005) and inertial fusion driven by ion and laser beams (Roth *et al*., 2005). Here the fast ignition concept calls for a detailed analysis of energy deposition processes in a dense plasma environment (Barriga-Carrasco & Maynard, 2005; Leon *et al*., 2005; Doria *et al*., 2004). New highly efficient and high resolution X-ray detection methods allow following the energy loss process of heavy ions inside targets and drawing conclusions of the charge state and energy loss dynamics (Rosmej *et al*., 2005).

One more application that comes to mind from these types of studies is that of a plasma diagnostic in laser plasma interaction studies.

ACKNOWLEDGMENTS

This work was partially supported by the German Israeli Project Cooperation Foundation (DIP). The authors are very thankful to Prof. Y. Maron for many valuable comments.

REFERENCES

Arad, R., Tsigutkin, K., Ralchenko, Yu.V. & Maron, Y. (2000). Spectroscopic investigations of a dielectric-surface-discharge plasma source. *Phys. Plasmas* **7**, 3797.

Assmann, W., Huber, H., Karamian, S.A., Grüner, F., Mieskes, H.D., Andersen, J.U., Posselt, M. & Schmidt, B. (1999). Transverse cooling or heating of channeled ions by electron capture and loss. *Phys. Rev. Lett.* **83**, 1759.

Barriga-Carrasco, M. .D. . & Maynard, G. (2005). A 3D trajectory numerical simulation of the transport of energetic light ion beams in plasma targets. *Laser Part. Beams* **23**, 211.

Betz, H.D. (1981). Heavy ion charge states. In *Applied Atomic Collision Physics*. Vol. 4, p. 1. New York: Academic Press.

Bohr, N. & Lindhard, J. (1954). Electron capture and loss by heavy ions penetrating through matter. *K. Dan. Vidensk. Selsk. Mat. Fys. Medd.* **28** (7), 1–30.

Dietrich, K.-G., Hoffmann, D.H.H., Boggasch, E., Jacoby, J., Wahl, H., Elfers, M., Haas, C.R., Dubenkov, V.P. & Golubev, A.A. (1992). Charge state of fast heavy ions in a hydrogen plasma. *Phys. Rev. Lett.* **69**, 3623.

Doria, D., Lorusso, A., Belloni, F., Nassisi, V., Torrisi, L. & Gammino, S. (2004). A study of the parameters of particles ejected from a laser plasma. *Laser Part. Beams* **22**, 461.

DuBios, R.D. et al. (2004). Electron loss from 1.4-MeV/u $U^{4,6,10+}$ ions colliding with Ne N_2 and Ar targets. *Phys. Rev. A* **70**, 032712.

Fisher, D.V. & Maron, Y. (2002). Effective statistical weights of bound states in plasmas. *Eur. Phys. J. D*, **18**, 93.

Fisher, D.V. & Maron, Y. (2003). Characterization of electron states in dense plasmas and its use in atomic kinetics modeling. *J. Quant. Spectr. Rad. Transf.* **81**, 147.

Fortov, V.E. & Yakubov, I.V. (1990). *Physics of No Ideal Plasma*. New York: Hemisphere Publishers.

Gryzinski, M. (1965). Classical theory of atomic collisions. I:. Theory of inelastic collisions. *Phys. Rev. A* **138**, 336.

Hoffmann, D.H.H., Weyrich, K. & Wahl, H. (1990). Energy loss of heavy ions in a plasma target *Phys. Rev. A* **42**, 2313.

Hoffmann, D.H.H., Blazevic, A., NI, P., Rosmej, O., Roth, M., Tahir, N.A., Tauschwitz, A., Udrea, S., Varentsov, D., Weyrich, K. & Maron, Y. (2005). Present and future perspectives for high energy density physics with intense heavy ion and laser beams. *Laser Part. Beams* **23**, 47.

Jacoby, J., Hoffmann, D.H.H., Laux, W., Müller, R.W., Wahl, H., Weyrich, K., Boggasch, E., Heimrich, B., Stöckl, C, Wetzler, H. & Miyamoto, S. (1995). Stopping of Heavy Ions in a Hydrogen Plasma. *Phys. Rev. Lett*., **74**, 1550.

Knudsen, H., Haugen, H.K. & Hvelplund, P. (1981). Single-electron-capture cross-section for medium- and high-velocity, highly charged ions colliding with atoms. *Phys. Rev. A* **23**, 597.

Lapicki, G. & McDaniel, F.D. (1980). Electron capture from *K* shells by fully stripped ions. *Phys. Rev. A* **22**, 1896.

Leon, P.T., Eliezer, S., Jose, M.P. & Martinez-Val, M. (2005). Inertial fusion features in degenerate plasmas. *Laser Part. Beams* **23**, 193.

Maynard, G., Chabot, M. & Gardes, D. (2000). Density effect and charge dependent stopping theories for heavy ions in the intermediate velocity regime. *Nucl. Instr. Meth. B* **164–165**, 139–146.

Maynard, G. (2002). Swift heavy ions in dense plasmas: The

interaction process as a probe of the plasma properties. *Laser Part. Beams* **20**, 467.

McGuire, J.H. & Richard, P. (1973). Procedure for computing cross-sections for single and multiple ionization of atoms in the binary-encounter approximation by the impact of heavy charged particles. *Phys. Rev. A* **8**, 1374.

Mueller, D., Grisham, L., Kaganovich, I., Watson, R.L., Horvat, V. & Zaharakis, K.E. (2001). Multiple Electron Stripping of 3.4 MeV/u Kr^{7+} and Xe^{11+} in Nitrogen. *Phys. Plasmas* **8**, 1753.

Mueller, D., Grisham, L., Kaganovich, I., Watson, R.L., Horvat, K.E., Zaharakis, K.E. & Peng, Y. (2002). Multiple electron stripping of heavy ion beams. *Laser Part. Beams* **20**, 551.

Meyerhof, W.E., Anholt, R.J., Eichler, J., Gould, H., Munger, Ch., Alonso, J., Thieberger, P. & Wegner, H.E. (1985). Atomic collisions with relativistic heavy ions. III: Electron capture. *Phys. Rev. A* **32**, 3291.

Meyerhof, W.E., Anholt, R., Xu, X.-Y., Gould, H., Feinberg, B., McDonald, R.J., Wegner, H.E. & Thieberger, P. (1987). Multiple ionization in relativistic heavy-ion–atom collisions. *Phys. Rev. A* **35**, 1967.

Nardi, E. & Zinamon, Z. (1982). Charge state and slowing of fast ions in plasma. *Phys. Rev. Lett.* **49**, 1251.

Nardi, E., Zinamon, Z., Tombrello, T.A. & Tanushev, N. (2002). Simulation of the interaction of high energy C_{60} cluster ions with amorphous targets. *Phys. Rev. A* **66**, 013201.

Nikolaev, V.S. (1967). Calculation of the effective cross-sections for proton charge exchange in collisions with multi-electron atoms. *JETP* **24**, 847.

Ralchenko, Yu.V. & Maron, Y. (2001). Accelerated recombination due to resonant deexcitation of metastable states. *J. Quant. Spectr. Rad Transf.* **71**, 609.

Richard, P. (1985). *Atomic Inner Shell Processes I* (Crassman, B., ed.), p. 73. New York: Academic.

Rosmej, O.N., Pikuz, S.A., Korostiy, S., Blazevic, A., Brambrink, E., Fertman, A., Mutin, T., Efremov, V.P., Pikuz, T.A., Faenov, A.Ya., Loboda, P., Golubev, A.A., Hoffmann, D.H.H. (2005). Radiation dynamics of fast heavy ions interacting with matter. *Laser Part. Beams* **23**, 79.

Roth, M., Stöckl, C., Süss, W., Iwase, O., Gericke, D.O., Bock, R., Hoffmann, D.H.H., Geissel, M. & Seelig, W. (2000). Energy loss of heavy ions in laser-produced plasmas. *Europhys. Lett.* **50**, 28.

Roth, M., Brambrink, E,. Audebert, P., Blazevic, A., Clarke, R., Cobble, J., Cowan, T.E., Fernandez, J., Fuchs, J., Geissel, M., Habs, D., Hegelich, M., Karsch, S., Ledingham, K., Neely, D., Ruhl, H., Schlegel, T. & Schreiber, J. (2005). Laser accelerated ions and electron transport in ultra-intense laser matter interaction. *Laser Part. Beams* **23**, 95.

Rozet, J.P., Stephan, C. & Vernhet, D. (1996). ETCHA: A program for calculating charge states at GANIL energies. *Nucl. Instr. Meth. B* **107**, 67.

Shevelko, V.P., Tolstikhina, I.Yu. & Stohlker, Th. (2001). Stripping of fast heavy low-charged ions in gaseous targets. *Nucl. Instr. Meth. B* **184**, 295.

Sols, F. & Flores, F. (1989). Inelastic cross-sections and charge states for B, C, N, and O ions moving in metals. *Phys. Rev. A* **37**, 1469.

Stockl, C., Boine-Frankenheim, O., Geissel, M., Roth, M.,Wetzler, H., Seelig, W., Iwase O., Spiller, P., Bock, R., Süss, W. & Hoffmann, D.H.H. (1998). Experiments on the interaction of heavy ions with dense plasma at GSI-Darmstadt. *Nucl. Instr. Meth. A* **415**, 558.

Xu, X.-Y., Montenegro, E.C., Anholt, R., Danzmann, K., Meyerhof, W.E., Schlachter, A.S., Rude, B.S. & McDonald, R.J. (1988). Intermediate-velocity atomic collisions. II. *K*-shell ionization and excitation in 8.6-MeV/amu Ca ions. *Phys. Rev. A* **38**, 1848.

Zimmerman, G.B. & More, R.M. (1980). Pressure ionization in laser fusion target simulations. *J. Quant. Spectr. Rad Transf.* **23**, 517.